Negative-Sequence Differential Protection – Principles, Sensitivity, and Security

Bogdan Kasztenny, Normann Fischer, and Héctor J. Altuve
Schweitzer Engineering Laboratories, Inc.

This paper was presented at the 68th Annual Conference for Protective Relay Engineers and can be accessed at: http://dx.doi.org/10.1109/CPRE.2015.7102180.

For the complete history of this paper, refer to the next page.

Presented at the
69th Annual Georgia Tech Protective Relaying Conference
Atlanta, Georgia
April 29–May 1, 2015

Previously presented at the
68th Annual Conference for Protective Relay Engineers, March 2015

Originally presented at the
41st Annual Western Protective Relay Conference, October 2014

Negative-Sequence Differential Protection – Principles, Sensitivity, and Security

Bogdan Kasztenny, Normann Fischer, and Héctor J. Altuve, *Schweitzer Engineering Laboratories, Inc.*

***Abstract*—This paper explains the principles of negative-sequence differential (87Q) protection, its basis for excellent sensitivity and speed, and the need for securing it with external fault detectors to deal with the saturation of current transformers. The paper reviews applications of 87Q elements to lines and transformers. It explains why 87Q elements cannot be used for turn-to-turn fault protection in shunt reactors and stators of generators and motors. The paper presents applications of negative-sequence directional elements for turn-to-turn fault protection in reactors and stators. Finally, it derives two new protection principles based on negative sequence for generator turn-to-turn fault protection.**

I. Introduction

In the field of power system protection, we encounter situations when a short circuit causes a small or no fault current flow at the terminals of the protected apparatus. These cases require protection elements of high sensitivity so that all faults are promptly cleared, reducing further damage to the protected apparatus and limiting danger to the public and the environment. These cases include the following:

- Faults on transmission lines with high resistance due to poor tower grounding or fault resistance.
- Turn-to-turn faults in power transformers, autotransformers, and phase-shifting transformers.
- Turn-to-turn and ground faults in stators of generators and motors.
- Turn-to-turn faults in shunt reactors.
- Capacitor failures in shunt capacitor banks.

Negative-sequence differential (87Q) protection has been applied to line protection for more than a decade [1]. Recently, it has been applied to transformer protection, primarily for its sensitivity to turn-to-turn faults [2] [3] [4].

The 87Q elements follow the current differential principle, but apply it to the calculated negative-sequence components of the zone currents, rather than to the measured phase currents. As a result, 87Q elements effectively operate on incremental quantities that respond to fault conditions. They are not affected by balanced prefault load and, therefore, should be more sensitive than phase differential (87P) elements.

Generally, across many protection principles and applications, the negative-sequence-based elements are more sensitive than the phase current-based elements. However, in the case of differential protection, the phase operating signals (differential signals) are already incremental quantities (i.e., they develop in response to an internal fault and do not contain any load current components).

The 87Q differential signal is a sum of the negative-sequence components of the zone currents. As such, it is identical to the negative-sequence component of the phase differential signals, and the 87Q operating signal becomes elevated only if the 87P operating signals are elevated. The enhanced sensitivity of 87Q elements does not come from the operating signal, but from the way 87Q elements are restrained. However, if restraining is the key to sensitivity, we can achieve arbitrarily high sensitivity from 87P elements by reducing their restraining action, such as by lowering the slope setting.

In this paper, we ask the following questions: Are 87Q elements really more sensitive than 87P elements? What is the real source of 87Q sensitivity? What is the best way to secure 87Q elements against current measurement errors?

Section II of this paper addresses these questions by providing an in-depth analysis of 87Q protection in general. Section III and Section IV review applications of 87Q elements to lines and power transformers.

Good performance of the 87Q elements in line and transformer applications invites the following question: Can this principle be successfully applied for turn-to-turn fault protection of stators and reactors? Turn-to-turn faults produce little or no differential current at the terminals of the protected apparatus. Section V explains why the 87Q element does not detect turn-to-turn faults in reactors and stators.

Section VI presents applications of negative-sequence directional (32Q) elements for turn-to-turn fault protection in stators and reactors.

Section VII introduces two novel protection principles for turn-to-turn fault protection for synchronous generator stators and rotors, utilizing the negative-sequence stator current and the double-frequency field current.

II. Principles of 87Q Protection

With reference to Fig. 1, the 87Q element follows the differential protection principle using the negative-sequence components of all zone currents. For each zone terminal *n*, the phase currents (i_{nA}, i_{nB}, i_{nC}) are filtered to obtain the fundamental frequency phasors (I_{nA}, I_{nB}, I_{nC}), from which the negative-sequence components (I_{nQ}) are calculated and added to form the operating (differential) signal:

$$I_{DIF(Q)} = \left| I_{1Q} + I_{2Q} + ... + I_{NQ} \right| \quad (1)$$

When the percentage differential characteristic is used, a companion restraining signal is created using (2):

$$I_{RST(Q)} = k \bullet \left(\left| I_{1Q} \right| + \left| I_{2Q} \right| + ... + \left| I_{NQ} \right| \right) \quad (2)$$

where *k* is a multiplying factor.

In its simplest version, the 87Q element operates when the differential signal is above a fixed pickup threshold (P) and above a fraction (percentage slope, S) of the restraining signal, as defined in (3):

$$\left(I_{DIF(Q)} > P \right) \text{ and } \left(I_{DIF(Q)} > \frac{S}{100} \bullet I_{RST(Q)} \right) \quad (3)$$

Practical implementations sometimes use more complex operating logic, such as a switched slope, upon external fault detection for better security under current transformer (CT) saturation.

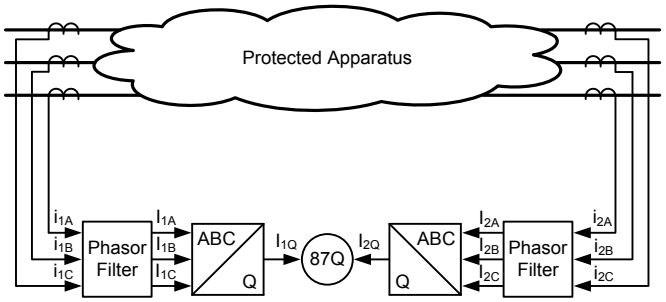

Fig. 1. Principle of 87Q protection.

Before we look at the details of the operating logic, we examine the operating and restraining signals in more detail.

A. 87Q Operating Signal

It is beneficial to realize that the 87P and 87Q operating signals are related. The 87P operating signals are per-phase sums of the phase zone currents (Fig. 2a). The 87Q operating signal is the sum of the negative-sequence components of all the phase zone currents (Fig. 2b). However, because the sum and negative-sequence operations are linear, we obtain exactly the same value applying the negative-sequence operation first and the summation later (Fig. 2b) as when applying the summation first and the negative-sequence operation later (Fig. 2a).

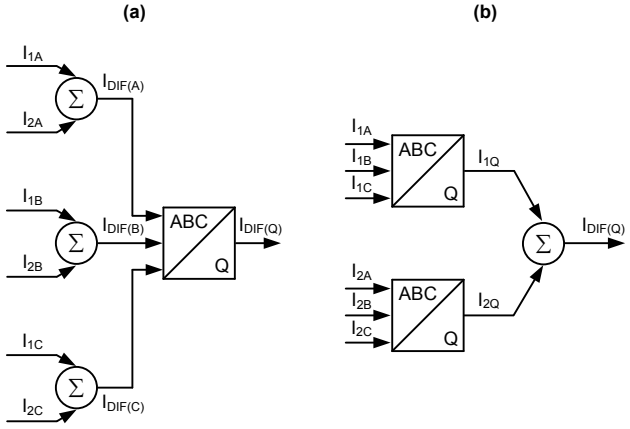

Fig. 2. 87P and 87Q operating signals are related; the (a) and (b) methods of deriving the 87Q operating signal are equivalent.

As a result, the 87Q operating signal is nothing more than the negative-sequence component of the 87P operating signals.

This key observation allows us to conclude the following:

- The 87Q operating signal is just a phase unbalance component of the 87P operating signals, and it will not show non-zero values for internal faults unless the 87P operating signals show non-zero values. We cannot expect the 87Q operating signal to be higher than the 87P operating signals.
- Conditions that lead to spurious 87P operating signals (such as CT saturation or transformer inrush current) will lead to a spurious 87Q operating signal as well.
- Conditions that lead to standing but symmetrical 87P operating signals (tap changer ratio mismatch, line charging current, partial differential applications, and so on) will not result in a standing 87Q operating signal.
- Both 87P and 87Q operating signals are independent from load (current ratio mismatch notwithstanding).

At this point, we firmly conclude that the 87Q sensitivity does not stem from its operating signal. The amount of information in the 87P and 87Q operating signals is very similar. The two operating signals provide similar sensitivity for internal faults (operating is expected) and similar security concerns for noninternal fault conditions (restraining is expected).

B. 87Q Restraining Signal

Equation (2) is probably the most common way of calculating the restraining signal, but other alternatives are also possible [5]. All these methods of forming the restraint aim at creating a signal that reflects the external fault current flow through the zone CTs. This signal serves as a counterbalance to the spurious operating signal caused by CT saturation and other error sources.

When applied to negative-sequence currents (or zero-sequence currents) as compared with phase currents, the fundamental premise of the restraining signal is critically challenged as follows:

- The CTs carry phase currents, and it is the phase currents (not the negative-sequence component of the phase currents) that stress the CTs, causing saturation and errors. Using the negative-sequence component alone as a measure of potential CT saturation underestimates the danger of saturation.
- The negative-sequence component is an incremental quantity, typically zero or very small under normal conditions, producing no prefault restraining bias for the 87Q element.
- The negative-sequence current is very low for symmetrical or near-symmetrical faults, producing no effective restraint, while the phase currents impacting the CTs can be arbitrarily high during these faults.

These issues impact the 87Q element security, but at the same time, they are the source of its sensitivity, as we explain next.

Consider an internal and an external fault on a power line, as depicted in Fig. 3a and Fig. 3b, respectively.

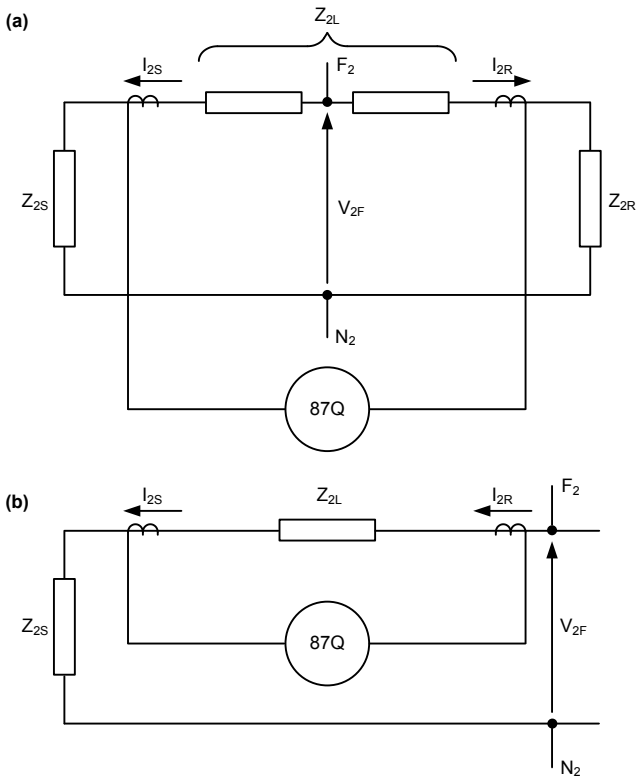

Fig. 3. Negative-sequence network for internal (a) and external (b) faults on a power line.

Typically, the negative-sequence network is homogeneous, meaning the angles of the line (Z_{2L}) and the system (Z_{2S} and Z_{2R}) impedances are very similar. If so, the negative-sequence currents measured differentially at the line terminals are practically in phase for internal faults (Fig. 3a) and practically out of phase for external faults (Fig. 3b).

This phase relationship has an important implication. During internal faults, the operating signal (1) is the highest possible, given the fault voltage and all involved impedances, and equals the sum of all the negative-sequence current magnitudes. As a result, the ratio between the operating (1) and restraining (2) signals is always very close to 100 percent. This ensures the 87Q element dependability and sensitivity even for very conservative slope settings, such as 80 percent. Moreover, this relationship is independent from the load flow in the system. It is this property of the restraining signal that makes the 87Q element considerably more sensitive than the 87P element.

There are, however, conditions that can reduce the 87Q element sensitivity. The two most common ones are an open-pole condition causing a standing negative-sequence current and restraint [6] and the presence of series compensation making the negative-sequence network nonhomogeneous [7] and reducing the operating signal relative to the restraining signal for internal faults.

C. 87Q Security Under CT Saturation

The 87Q restraining signal alone is not able to properly secure the element under CT saturation. As explained previously, the phase currents are responsible for CT errors, and under near-balanced external faults, the phase currents can be high while the negative-sequence currents (and therefore the 87Q restraining signal) can be very small or even zero. Typical solutions for this problem include either CT saturation detection logic or external fault detection (EFD) logic.

The CT saturation detection logic typically delays the 87Q element so that it can measure the harmonics of the phase differential signals once the CTs saturate and use the high level of harmonics to either desensitize or entirely block the 87Q element [8].

The EFD logic asserts in response to external faults before and regardless of CT saturation. Therefore, the EFD logic does not require or depend on delaying the 87Q element. Fig. 4 shows a typical implementation used in line current differential, transformer differential, and bus differential elements [3] [6] [9]. The EFD operating principle takes advantage of the fact that CTs do not saturate instantaneously. As a result of the initial error-free CT operation, the phase restraining signal increases while the phase differential signal remains very small for external faults.

The logic of Fig. 4 uses incremental quantities (derived over a 1-cycle time span) to prevent the EFD from picking up on load currents [6]. The EFD asserts when the incremental signal derived from the restraining current (i_{RST}) becomes greater than some threshold value (P) and, at the same time, the incremental signal derived from the differential current (i_{DIF}) remains smaller than a percentage (q factor) of the restraining signal during a fraction (3/16) of the power cycle. Once the EFD picks up, it will remain in that state for the timer dropout time (DPO).

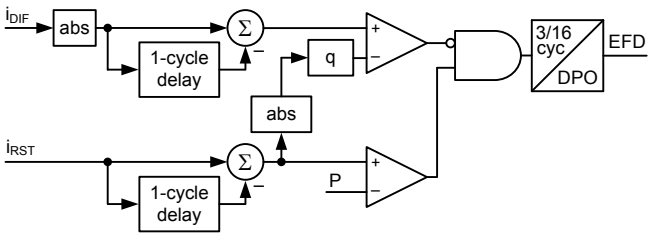

Fig. 4. Simplified logic diagram of ac EFD logic [6].

The logic of Fig. 4 detects high-current events that are not caused by internal faults and guards the differential elements (including the 87Q element) against CT saturation that happens because of the high ac component in the currents.

However, CT saturation can also happen because of a long-lasting dc component in the current, even though the current magnitude is not very high. This is often the case for generator protection relays during the inrush of a nearby transformer or for remote system faults (due to the very large X/R ratio near generators) [6]. To address this CT saturation scenario, dc EFD logic is used, as shown in Fig. 5.

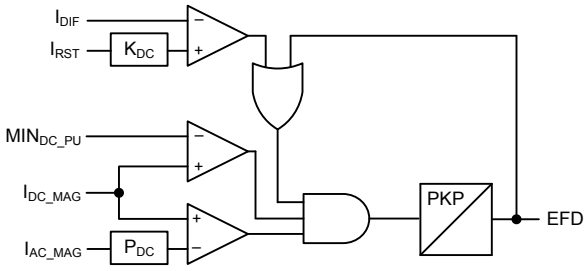

Fig. 5. Simplified logic diagram of dc EFD logic [9].

For detecting low-magnitude external events (faults or inrush) that have a long-decaying dc offset component, the dc EFD logic compares the fundamental frequency current magnitude (I_{AC_MAG}) with the dc component current magnitude (I_{DC_MAG}). A significant dc component is declared if the dc component is greater than a fixed portion (P_{DC}) of the ac component at the time. An external fault is declared if the current contains a significant dc component, the differential current (I_{DIF}) is less than the restraining current (I_{RST}) times a factory constant (K_{DC}), and this situation persists for several cycles (defined by the timer setting PKP).

The EFD logic diagrams shown in Fig. 4 and Fig. 5 are applicable to differential elements with any number of input currents and are typically applied to an OR gate to provide security for high-current and long dc decay scenarios.

87Q elements are sometimes blocked upon EFD assertion [3]. More typically, their security is increased—at the expense of some loss of sensitivity—in anticipation of possible CT saturation. This increase in security can include one or more of the following [6]:

- Increasing the slope value (S) applied to the restraining quantity in the operating logic (3). This solution, however, has a limited effect because the slope can be set permanently high (e.g., 80 percent) without jeopardizing sensitivity, as explained earlier, and it cannot be increased above 100 percent.
- Adding a portion of a phase restraining signal to the negative-sequence restraining signal. This is a very effective way of dealing with CT saturation during balanced faults that do not produce any significant natural negative-sequence restraint.
- Adding harmonics from the phase differential signals to the negative-sequence restraining signal. This is an effective way of dynamically increasing the restraint in response to the CTs actually saturating and producing spurious (and more importantly, distorted) phase differential signals.
- Adding extra time delay to ride through transient CT saturation and provide overall security for external faults.

It is worth emphasizing that the EFD logic presented in this paper will not trigger on internal faults, even if the CTs saturate. Therefore, the listed means of providing extra security will not be in place for internal faults and will not erode the natural sensitivity and speed of 87Q elements.

D. 87Q Element Speed Considerations

87Q elements are naturally very fast. This high operating speed results from the fact that, for internal faults, the operating and restraining signals are essentially equal, including the transition from the prefault value of zero to the fault value. This condition results from the homogeneity of the negative-sequence network, which causes all the involved terminal negative-sequence currents to be effectively in phase for internal faults. As a result, the fault trajectory on the $I_{DIF(Q)}$ versus $I_{RST(Q)}$ plane is approximately a straight line with a 100 percent slope (Fig. 6a). This, in turn, means that the trajectory crosses the restraining-blocking boundary on the operating characteristic through the minimum pickup line, because the slope setting is always lower than 100 percent. Because the minimum pickup is typically much smaller than the 87Q operating signal for an internal fault, the operation is very fast.

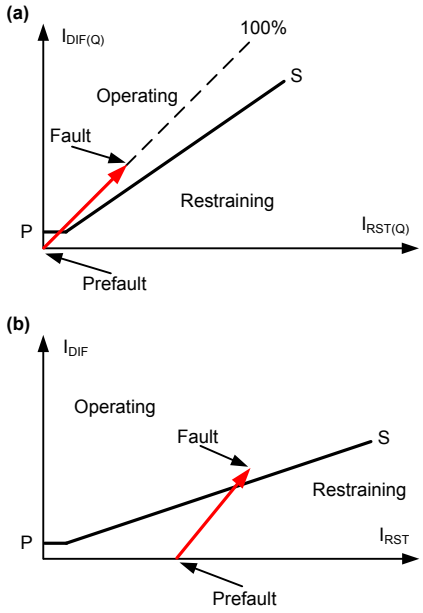

Fig. 6. Fault trajectories (in red) of the 87Q (a) and 87P (b) elements and their impact on speed of operation.

By contrast, the I_{DIF} versus I_{RST} trajectory for the 87P elements starts from a load-determined restraint and zero operating signal and moves to the right (the restraining signal increases) and upwards (the differential signal increases) on the operating characteristic until it crosses (or not) the slope line of the restraining-operating boundary, as shown in Fig. 6b. Depending on the severity of the fault, this transition can take a substantial portion of a power cycle (assuming typical 1-cycle filtering). In extreme cases, the 87P element may even fail to operate if its load-influenced restraint is too high given the magnitude of the operating signal.

In Fig. 6, the length of the trajectory line is equivalent to the length of the filtering window used. We will assume it is one power cycle. With reference to Fig. 6a, the 87Q operating point crosses the operating boundary after about 0.2 of the total filtering window length (i.e., after 0.2 cycle). With

reference to Fig. 6b, the 87P element responds in about 0.9 cycle to this marginal fault. The 87P element will operate faster for high-current faults, but it may fail to operate if the operating current is too low given the load-influenced restraining signal.

When secured with EFD logic, 87Q elements do not need to be delayed for security. However, because the 87Q element does not have any natural restraint and therefore any natural blocking bias in the prefault state (Fig. 6a), some implementations add a small security delay in the order of one power cycle.

III. 87Q Elements Increase Line Protection Sensitivity

Line current differential (87L) elements compare currents from the line terminals using a communications channel. 87L protection is secure and more dependable than all other line protection schemes in use today. It performs well for evolving, intercircuit, and cross-country faults; under power swings and open-pole conditions; and on series-compensated lines.

A. Challenges of 87L Protection

Challenges of 87L protection include the requirements of high sensitivity for internal faults and security for external faults with CT saturation, current alignment issues, limited channel bandwidth, channel impairments, and line charging current, among others.

In 87L applications, phase differential (87LP) elements face the following two challenges:

- The use of phase restraining currents limits 87LP element sensitivity, despite the fact that their differential signals are not impacted by load.
- The 87LP elements are prone to misoperation for external faults or even load currents if the currents are misaligned, such as when using the ping-pong synchronization method in applications over asymmetrical channels.

B. Advantages of 87Q Elements for Line Protection

Advantages of applying 87Q elements to line protection (87LQ) include the following:

- The load component is removed not only from the differential signal but also from the restraining signal, thus allowing for much higher sensitivity. The standing negative-sequence current is very low during normal system operation, which mitigates the effect of temporary current misalignment should it happen due to an asymmetrical channel.
- The negative-sequence network is typically very homogeneous, which keeps the negative-sequence currents of the line protection zone practically in phase for internal faults and practically out of phase for external faults.
- The 87LQ elements are less affected by line charging current than the 87LP elements.

C. 87LQ Element Alpha Plane Characteristic

In 87LQ protection, the current-ratio complex plane, or Alpha Plane, is a plot on a two-dimensional plane of the ratio of the remote negative-sequence current (I_{2R}) to the local negative-sequence current (I_{2L}):

$$k = \frac{I_{2R}}{I_{2L}} \tag{4}$$

The 87Q elements that operate based on the Alpha Plane principle continuously calculate the ratio (4) and compare this ratio with an operating characteristic defined on the Alpha Plane.

Fig. 7 is a representation of different power system events on the Alpha Plane [1] [6] [10]. Fig. 7 shows that the angular sector representing internal faults is narrower for the negative-sequence currents than for the phase currents. This is because the angle difference between the local and remote negative-sequence currents depends only on system nonhomogeneity, which is very low, and does not depend on the source voltages driving the phase currents, especially the positive-sequence current components. For simplicity, the figure does not show the angle rotation created by the current alignment errors. Under these errors, all the shapes in Fig. 7 would rotate clockwise or counterclockwise based on the sign and amount of asymmetrical delay between the two 87L relays.

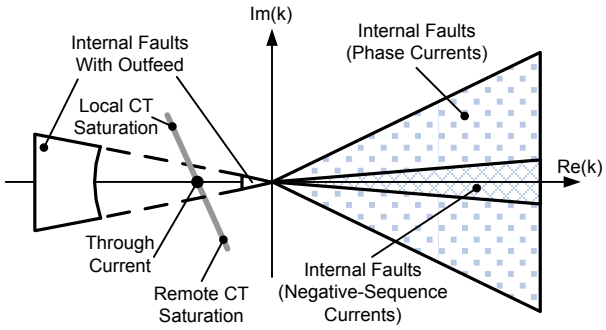

Fig. 7. Power system events on the Alpha Plane.

Fig. 8 shows a typical 87Q Alpha Plane characteristic for 87L protection applications. The characteristic has two settings: the blocking radius R and the blocking angle α [1] [10]. The differential element operates when the current ratio leaves the restraining region and the differential signal magnitude is above a minimum pickup value.

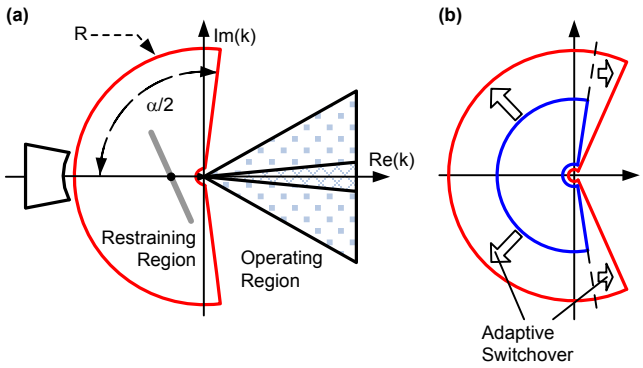

Fig. 8. Alpha Plane 87LQ element operating characteristic (a); adaptive Alpha Plane characteristic with normal and extended security settings (b).

The generalized Alpha Plane protection principle [6] [10] [11] extends the two-terminal principle (4) to multiterminal lines. The generalized Alpha Plane algorithm measures the currents that bound the differential zone, calculates differential and restraining auxiliary signals, and generates two equivalent currents in such a way that the two currents give the same differential and restraining signals as the actual multiterminal zone of 87L protection [6]. These equivalent currents plot an operating point on the equivalent Alpha Plane. This operating point is further checked against an Alpha Plane characteristic the same as in two-terminal applications.

As mentioned previously, 87Q elements are prone to misoperate on balanced external faults accompanied with CT errors. The EFD logic described in Section II, Subsection C solves this problem for 87L applications. The 87LQ elements based on the generalized Alpha Plane principle can apply the following adaptive measures upon assertion of the EFD:

- Increasing the blocking radius R, and/or the blocking angle α of the element characteristic (Fig. 8b).
- Adding a fraction of the maximum phase restraining signal to the negative-sequence restraining signal used for the generalized Alpha Plane calculations.
- Adding harmonics from the phase differential signals to the negative-sequence restraining signal.

87LQ elements secured by EFD or CT saturation detection logic provide excellent protection for transmission lines.

IV. Transformer Turn-to-Turn Fault Protection With 87Q Elements

The differential protection principle follows Kirchhoff's current law (KCL) in applications where a metallic per-phase connection exists between the terminals of the protected apparatus. These applications include buses, lines, generator and motor stators, and reactors. The sum of the terminal currents in each phase ideally equals zero for through-current conditions (i.e., no internal faults) and equals the fault current for internal faults that violate KCL for the protected apparatus.

Applications of current differential elements to power transformers are different. The individual windings of a power transformer are galvanically isolated (except in the case of autotransformers), and KCL cannot be directly applied. In transformer applications, the differential principle follows the ampere-turn (AT) balance between the core legs [12]. The sum of the ATs around any closed magnetic circuit loop ideally equals zero for transformer through-current conditions (i.e., no internal faults). This AT balance condition translates into zero differential signal in transformer 87P (87TP) and 87Q (87TQ) elements with proper ratio matching, vector group compensation, and zero-sequence removal [10]. An internal fault (including a turn-to-turn fault) upsets the AT balance and can be detected by 87TP or 87TQ elements.

A. Transformer Turn-to-Turn Faults Cause a Differential Signal

Fig. 9, taken from [12], shows a turn-to-turn fault (S closed) in the high-side (H) winding of a three-phase transformer with any winding connection and core type. In this figure, the dashed lines labeled 1, 2, and 3 represent the transformer core legs; *p* is the number of shorted turns (in per unit of the winding turns); and i_{FLT} is the fault current circulating in the faulted portion of the winding.

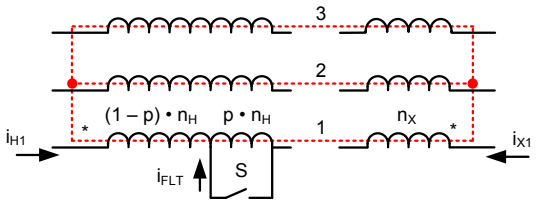

Fig. 9. A transformer turn-to-turn fault upsets the AT balance and causes a differential current.

The turn-to-turn fault changes the ATs on the affected core leg in an amount equal to the ATs produced by the fault current (i_{FLT}) flowing through the shorted turns ($p \bullet n_H$). As a result, the differential current reflects the unmonitored additional ATs produced by the turn-to-turn fault:

$$i_{DIF} \sim p \bullet n_H \bullet i_{FLT} \tag{5}$$

B. Challenges of Transformer Turn-to-Turn Fault Protection

In general, transformer turn-to-turn faults produce high current values in the shorted turns that can cause significant damage if not detected and isolated rapidly. On the other hand, faults involving a few turns produce a relatively small change in the terminal currents and therefore in the differential signal, which makes them difficult to detect.

An 87TP element may detect turn-to-turn faults if the transformer is lightly loaded (owing to a small restraining current). However, for high load conditions, the 87TP element sensitivity is reduced and its ability to detect turn-to-turn faults is diminished [3] [5].

C. Advantages of 87Q Elements for Transformer Turn-to-Turn Fault Protection

As mentioned previously, 87Q elements are highly sensitive and relatively independent from load. Therefore, they provide a sensitive way of detecting turn-to-turn faults.

In an 87TQ element, the differential signal is effectively the magnitude of the phasor sum of the appropriately shifted and ratio-matched negative-sequence components of the terminal currents. The vector group compensation shifts the negative-sequence current by an angle equal to the negative value of the vector group compensation angle [12]. For example, for a wye-delta transformer requiring a compensation angle of –30 degrees, the differential signal is:

$$I_{DIF(Q)} = \left| I_{X(Q)} + \frac{V_H}{V_X} \bullet e^{j30^\circ} \bullet I_{H(Q)} \right| \tag{6}$$

where subscripts H and X designate the transformer high- and low-voltage-side quantities, respectively.

As we explained in Section II, $I_{DIF(Q)}$, given by (6), is the negative-sequence component of the phase differential signals, so it does not provide any significant gain in sensitivity over the 87TP element. However, (6) is attractive when protecting phase-shifting transformers because it allows an arbitrary shift (not restricted to a multiple of 30 degrees) between the transformer windings [2].

The 87Q element sensitivity in transformer applications comes from the fact that the restraining signal does not include load current:

$$I_{RST(Q)} = \left|I_{X(Q)}\right| + \frac{V_H}{V_X} \bullet \left|I_{H(Q)}\right| \tag{7}$$

An 87TQ element defined by (6) and (7) is considerably more sensitive than 87TP elements for detecting transformer turn-to-turn faults. Reference [13] describes the experimental results of applying staged turn-to-turn faults to a three-phase, three-winding laboratory transformer. An 87TQ element was able to detect faults across 2, 4, 6, and 10 percent of transformer winding turns for different load conditions. The 87TP element failed to detect the 2 percent winding faults.

As in other applications, 87TQ elements must be secured by EFD or CT saturation detection logic for security under external faults with CT saturation. Also, they must be blocked for inrush conditions.

V. 87Q Limitations

As explained previously, differential protection follows KCL in applications to transmission lines (Section III) or it follows the AT balance in applications to power transformers (Section IV). In the former case, 87Q elements are able to detect internal faults because they cause current flow between the phases or to ground. In the latter case, 87Q elements are able to detect turn-to-turn faults because these faults upset the AT balance of the protected transformer.

We now examine if a differential element based strictly on KCL can detect turn-to-turn faults in stators or reactors or any other failure that does not create a current flow between phases or to ground. Fig. 10 presents a general application of the differential principle (87P and 87Q) to stators, shunt reactors, or capacitor banks.

Assume a turn-to-turn fault in Phase A or any other failure that changes the current, voltage, or flux in the protected apparatus but does not create a current flow between phases or to ground. Under this condition, based on KCL, the phase currents at both terminals of the protected apparatus match. Therefore:

$$\begin{aligned} &I_{2A} = I_{1A} \rightarrow I_{DIF(A)} = 0 \\ &I_{2B} = I_{1B} \rightarrow I_{DIF(B)} = 0 \rightarrow I_{DIF(Q)} = 0 \\ &I_{2C} = I_{1C} \rightarrow I_{DIF(C)} = 0 \end{aligned} \tag{8}$$

In other words, both the 87P and 87Q elements will fail to detect failures that do not cause any current flow between the phases or to ground.

In the case of stator and reactor protection, a turn-to-turn fault upsets the AT balance of the protected apparatus, but the differential scheme of Fig. 10 does not monitor that balance, and therefore, it will not operate. The turn-to-turn fault does create a negative-sequence unbalance, but the negative-sequence current flows through the protected apparatus, creating zero differential signal per (8).

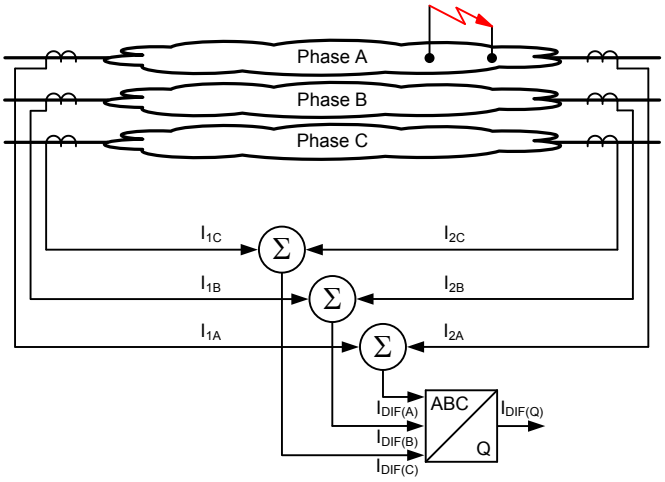

Fig. 10. Differential protection based strictly on KCL.

In the case of a capacitor bank, the shorted or opened capacitor units create an unbalance in the impedances and result in a negative-sequence current flow. Here, too, the negative-sequence current flows through the capacitor bank, resulting in zero differential signal per (8).

As a result, differential protection does not respond to turn-to-turn faults in stators [14] or reactors [15] or to capacitor failures in shunt capacitor banks. Instead, the following protection methods are typically relied upon:

- Split-phase protection is used in large hydroelectric generators for the detection of turn-to-turn faults. In other types of machines without the advantage of split windings, the stator is often left unprotected against turn-to-turn faults. These faults are considered unlikely, and if they happen, they need to evolve to ground or phase faults to be detected [16].
- Sudden pressure relays are used to protect oil-immersed reactors against turn-to-turn faults [15] [17].
- Unbalance protection methods designed to monitor changes in capacitor bank impedances are used for capacitor bank protection. These methods include phase and neutral voltage differential schemes and phase and neutral current unbalance schemes [18] [19].

Turn-to-turn faults in stators and reactors, as well as capacitor failures, do create a negative-sequence unbalance. In the next section, we explore the opportunity to use the negative-sequence quantities for protection.

VI. Application of 32Q Elements for Turn-to-Turn Fault Protection of Stators and Reactors

Consider the negative-sequence current and voltage at the terminals of a generator or motor stator, shunt reactor, or shunt capacitor bank. Consider further a system fault or other

external unbalance (Fig. 11a) and an internal fault or other internal unbalance (Fig. 11b).

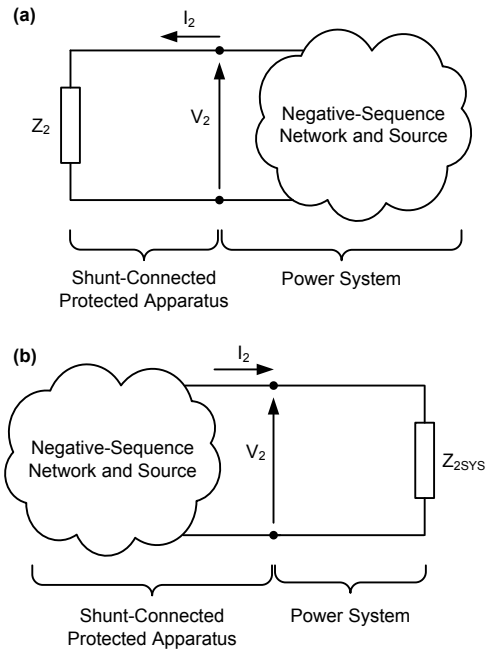

Fig. 11. Terminal current and voltage during system (a) and protected apparatus (b) faults and other unbalances.

During system unbalances (including short circuits and open-phase conditions), the negative-sequence source is on the system side of the apparatus CTs. This source creates a current flow that closes back through the impedance of the stator, reactor, or capacitor bank, creating a proportional negative-sequence voltage drop measured by the relay. As a result, the apparent negative-sequence impedance measured at the terminals of the protected apparatus during system unbalances is:

$$Z_2 = -Z_{2GEN} \text{ for generators} \quad (9)$$

$$Z_2 = +Z_{2REA} \text{ for reactors} \quad (10)$$

$$Z_2 = +Z_{2CAP} \text{ for capacitors} \quad (11)$$

The different signs reflect the typical CT polarity convention (looking into the reactor or capacitor bank and looking into the system in generator protection).

During unbalanced conditions in the protected apparatus, the negative-sequence source is on the apparatus side of the CTs. This source drives the negative-sequence current that closes through the negative-sequence system impedance, creating a proportional negative-sequence voltage drop measured by the relay. As a result, the apparent negative-sequence impedance measured at the terminals during unbalances in the protected apparatus is:

$$Z_2 = +Z_{2SYS} \text{ for generators} \quad (12)$$

$$Z_2 = -Z_{2SYS} \text{ for reactors and capacitors} \quad (13)$$

As expected, the apparent impedance plots in opposite quadrants for the system and protected apparatus unbalances, as depicted in Fig. 12 for the case of a generator.

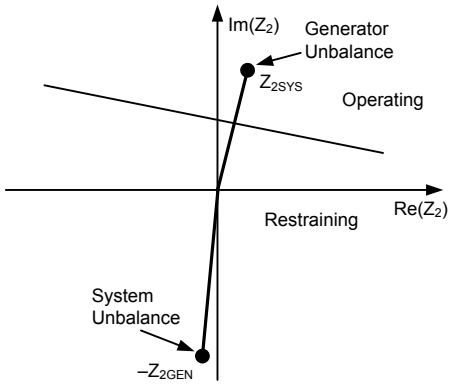

Fig. 12. Apparent negative-sequence impedance during system unbalances and generator unbalances, including stator turn-to-turn faults.

Normally, to use this apparent negative-sequence impedance polarity for tripping, we need to compare the fault direction at both terminals of the protected apparatus to make sure the fault is not beyond the opposite terminal of the protected apparatus. This is not the case for generator, motor, shunt reactor, or shunt capacitor protection, because these elements are not connected in series with any other apparatus but create the edges of the negative-sequence network. Therefore, we can use simple negative-sequence directional (32Q) elements for tripping for unbalances in these elements, as shown in Fig. 12.

In order to illustrate the 32Q application to stator turn-to-turn fault protection, we simulated external faults and internal turn-to-turn faults in a sample 13.8 kV, 200 MW machine using the Real Time Digital Simulator (RTDS®) [20]. The generator and system negative-sequence impedances are about 0.22 ohms and 0.1 ohms, respectively, both primary and as seen from the 13.8 kV generator terminals.

Fig. 13 shows terminal voltages and currents for an external phase-to-phase fault at the system side of the generator step-up transformer. Fig. 14 shows the negative-sequence impedance measured by the relay. As expected, the impedance trajectory settles in the third quadrant (compare to Fig. 12) at a value equal to the generator negative-sequence impedance.

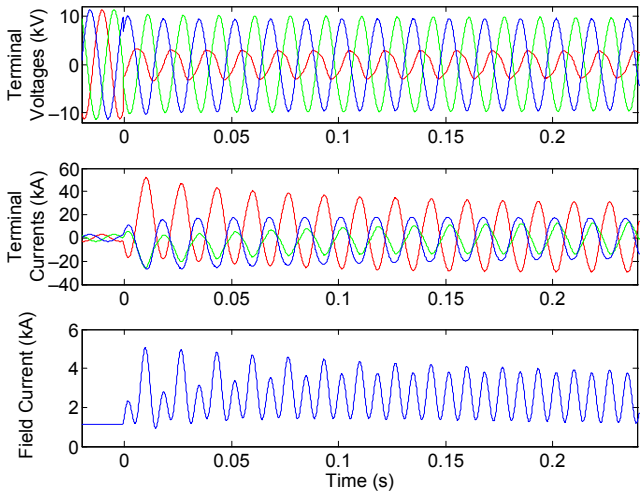

Fig. 13. External fault: terminal voltages and currents and field current.

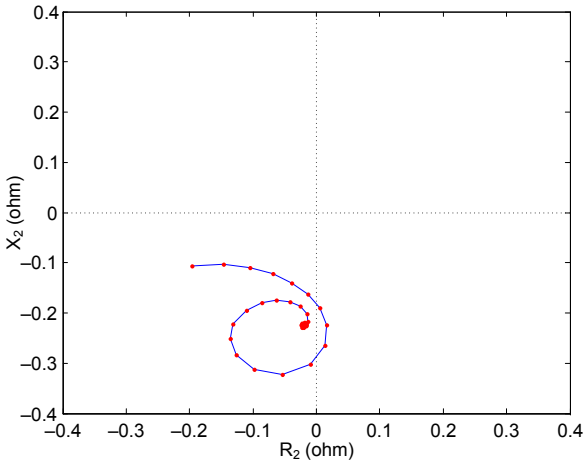

Fig. 14. Negative-sequence impedance measured at the generator terminals for the external fault of Fig. 13.

Fig. 15 shows a 5 percent turn-to-turn fault while the machine was loaded to 200 MW. A 5 percent turn-to-turn fault is the lowest percentage turn-to-turn fault that can be modeled in the RTDS. Fig. 16 shows the measured apparent negative-sequence impedance. As expected, the impedance trajectory settles in the first quadrant (compare to Fig. 12) at a value equal to the system negative-sequence impedance.

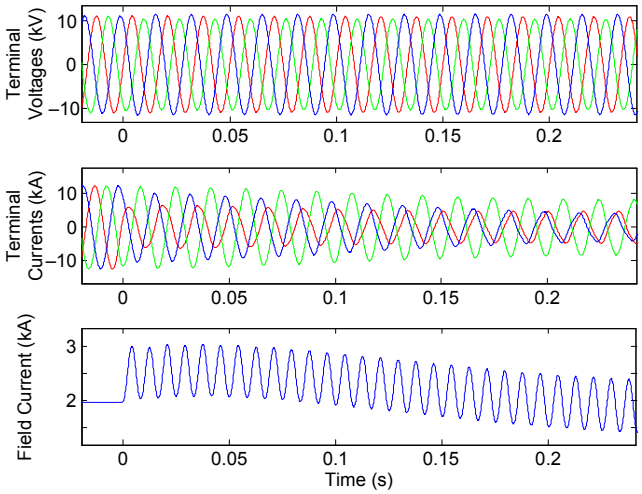

Fig. 15. Turn-to-turn fault: terminal voltages and currents and field current.

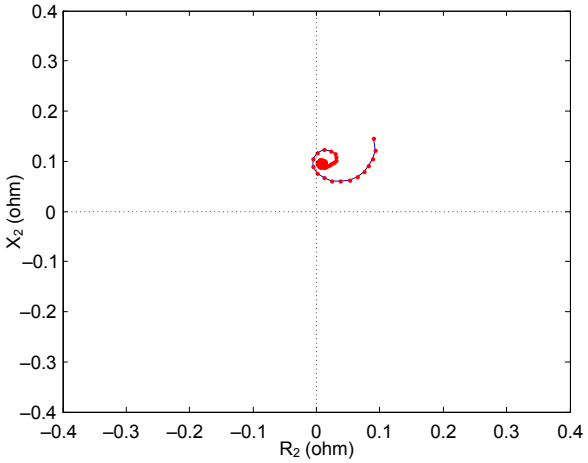

Fig. 16. Negative-sequence impedance measured at the generator terminals for the turn-to-turn fault of Fig. 15.

Of course, 32Q elements do not work for capacitor banks because the impedance of the bank is capacitive (negative) and therefore located in the same quadrant as the system impedance. Fortunately, reliable unbalance protection methods for capacitor banks are available today [18].

VII. Stator-Rotor Differential Elements

A. Fundamentals

The negative-sequence current in the stator creates a rotating magnetic field in the direction opposite to the rotor spin. As a result, the negative-sequence current induces double-frequency currents in the field winding and other parts of the rotor, including the damper windings (if any) and the rotor core surface. In our analysis, we lump the double-frequency currents flowing in other parts of the rotor into one current, called the damper current, that flows on an equivalent damper winding. When looking at the machine from the stator side and considering the negative-sequence current, we can view the generator as a three-winding rotating transformer, having the stator winding fed with the negative-sequence current, the damper winding fed with a double-frequency current, and the field winding also fed with a double-frequency current, as depicted in Fig. 17a.

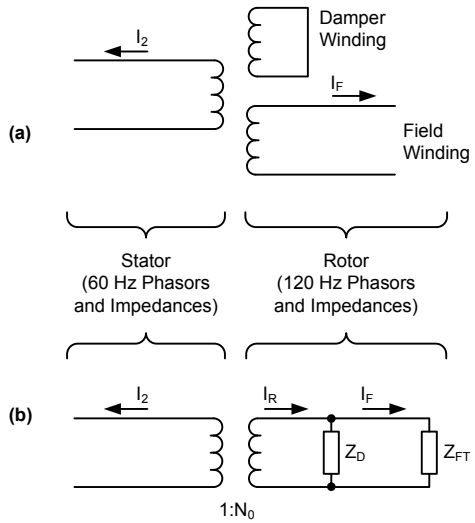

Fig. 17. An equivalent three-winding transformer relating the negative-sequence stator current and the double-frequency components of the field and damper currents (a); two-winding representation with the field and damper windings brought to the same voltage base (b).

We can provide turn-to-turn fault protection for stators and rotors by applying the AT balance to the equivalent three-winding transformer in Fig. 17a. We can measure the stator negative-sequence current and the field double-frequency current. However, we will never be able to measure the damper current. We can overcome this obstacle by examining Fig. 17b, in which we convert the damper and field impedances to the same voltage base and connect the two circuits in parallel to form a single equivalent winding. This way, we reduce the three-winding transformer to an equivalent two-winding transformer.

We assume the exciter does not produce any double-frequency voltage, and therefore, the field winding can be

considered shorted with the total impedance of the field winding and the exciter circuit, Z_{FT}. Z_D is the damper winding leakage impedance. The Z_D and Z_{FT} impedances are double-frequency (120 Hz) impedances and are brought to the same voltage base.

Fig. 17b shows that we can provide turn-to-turn fault protection by applying the AT balance between the negative-sequence current (I_2) in the stator and the total rotor current (I_R). Again, we cannot measure the total rotor current. However, as long as the damper impedance (Z_D) and the total field circuit impedance (Z_{FT}) are constant, we can calculate the total rotor current (I_R) from the measured field current (I_F):

$$I_R = I_F \bullet \left(1 + \frac{Z_{FT}}{Z_D}\right) \tag{14}$$

The phasors and impedances in (14) are double-frequency (120 Hz) quantities.

Assuming the turn ratio of the equivalent two-winding transformer is N_0, the AT balance condition for any external unbalance in a healthy generator is:

$$I_2 = N_0 \bullet I_R = N_0 \bullet I_F \bullet \left(1 + \frac{Z_{FT}}{Z_D}\right) \tag{15}$$

In other words, for any external unbalance, including faults, the ratio N_{SF} of the magnitudes of the negative-sequence stator current and the double-frequency rotor current for a healthy machine is:

$$N_{SF} = \left|\frac{I_2}{I_F}\right| = N_0 \bullet \left|1 + \frac{Z_{FT}}{Z_D}\right| \tag{16}$$

A turn-to-turn fault in the rotor or stator will upset the AT balance conditions (15) and (16), which allows the detection of such faults.

In order to test this hypothesis, we look at the I_2/I_F magnitude ratio for the external fault case of Fig. 13. Fig. 18 shows the two current magnitudes and their ratio. The I_2/I_F magnitude ratio settles at about 13.4 for this external unbalance.

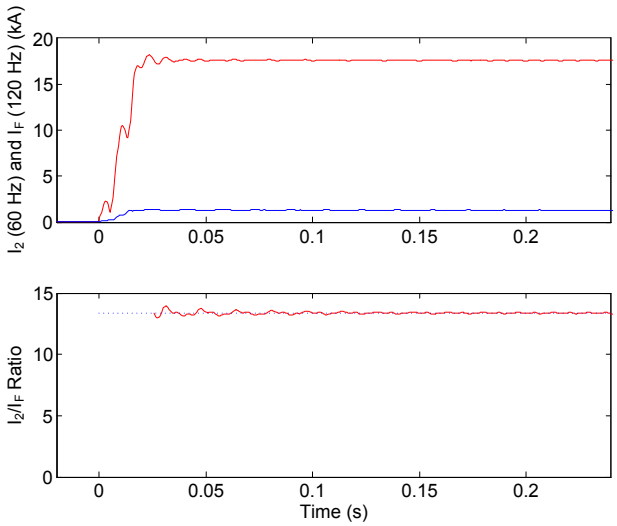

Fig. 18. External fault of Fig. 13: negative-sequence current magnitude (60 Hz) in red, field current magnitude (120 Hz) in blue, and magnitude ratio.

The 13.4 ratio for this particular machine should apply to any external unbalance. We tested this premise by simulating a number of external faults with the I_2 magnitude varying between 175 A and about 17 kA. Fig. 19 shows these external faults as red dots on the I_2 versus I_F current magnitude plane. As we can see, all the external fault cases plot as a straight line with a slope of 13.4.

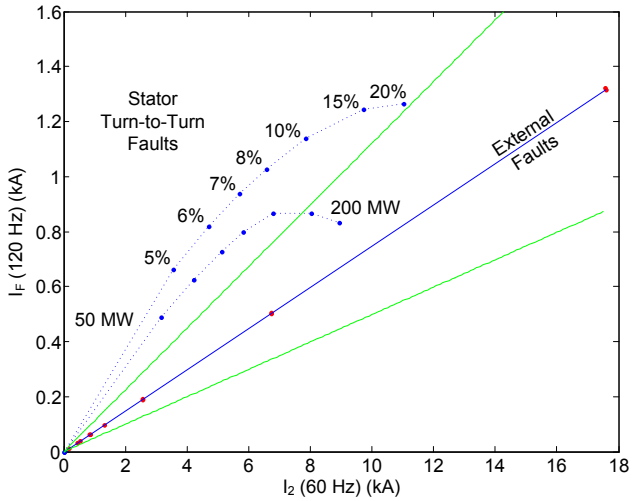

Fig. 19. Negative-sequence stator current magnitude versus double-frequency field current magnitude for external faults (red dots) and turn-to-turn faults (blue dots).

Having concluded that the I_2/I_F magnitude ratio holds constant for external faults, we now direct our attention to turn-to-turn faults. Fig. 20 shows the key signals for the simulated 5 percent turn-to-turn fault of Fig. 15. Note that for this fault, the I_2/I_F magnitude ratio is about 6 (compared with 13.4 for a healthy machine). In other words, instead of having an I_F magnitude of about 3 kA/13.4 = 220 A for I_2 = 3 kA, the machine exhibits an I_F magnitude of about 500 A. Such a significant difference allows us to detect this turn-to-turn fault very reliably.

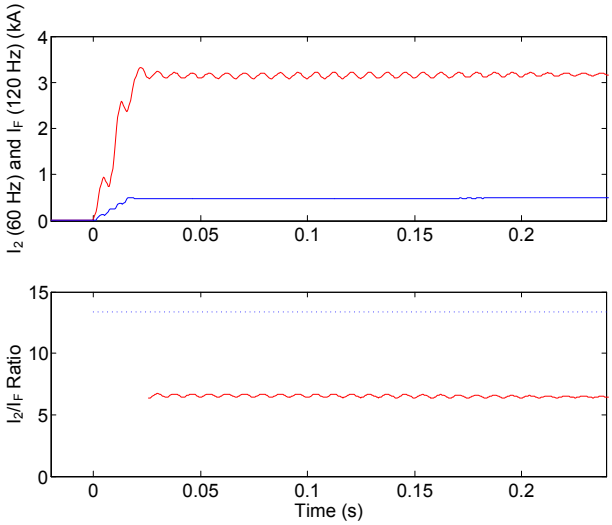

Fig. 20. Turn-to-turn fault of Fig. 15: negative-sequence current magnitude (60 Hz) in red, field current magnitude (120 Hz) in blue, and magnitude ratio.

Fig. 19 shows the plot of a number of turn-to-turn faults on the I_2 versus I_F current magnitude plane for generator loads of

50 MW and 200 MW. As we can see, these faults are located away from the straight line of external faults. The magnitude of I_F we measure depends on the machine load and is higher for a lightly loaded machine. Even for a fully loaded machine, the I_2/I_F magnitude ratio for turn-to-turn faults involving less than 10 percent of the turns differs by about 100 percent compared with the healthy machine. For faults involving 20 percent or more of the turns, the ratio is a less effective decision factor, especially for a heavily loaded machine, but these faults are very unlikely and can be reliably detected by the 32Q element.

Note that the 5 percent turn-to-turn faults plot considerably away from the line of external faults. We know that for turn-to-turn faults approaching 0 percent of shorted turns, there is no negative-sequence current in the stator or double-frequency current in the field winding. Therefore, we can extrapolate the dashed lines in Fig. 19 toward the origin of the plot. By doing so, we can see that the outlined principle will work well for turn-to-turn faults involving much less than 5 percent of the turns (the RTDS model we used is limited to 5 percent of the turns as the minimum turn-to-turn fault [20]).

B. Stator-Rotor Current Unbalance (60SF) Element

Based on the principle derived above, we propose a new protection element: the stator-rotor current unbalance (60SF) element. As shown in Fig. 21, the element measures the stator currents to calculate the negative-sequence stator current magnitude. It measures the field current (using a shunt, for example) to calculate the double-frequency field current magnitude.

The 60SF element applies the effective transformation ratio (N_{SF}) to match the magnitudes and checks if the two current magnitudes balance.

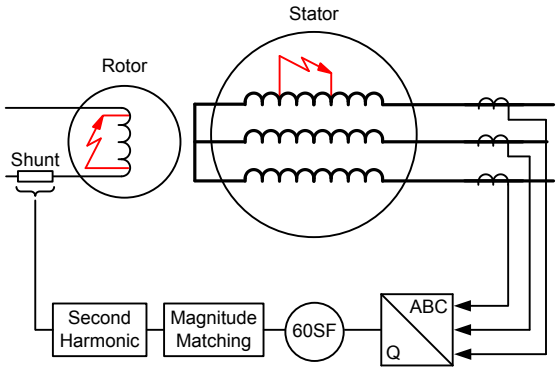

Fig. 21. The 60SF turn-to-turn fault protection element for synchronous generators.

A simple implementation of this 60SF element uses the following operating signal:

$$I_{OP} = \left| |I_{2(60Hz)}| - N_{SF} \bullet |I_{F(120Hz)}| \right| \quad (17)$$

and the following restraining signal:

$$I_{RST} = |I_{2(60Hz)}| + N_{SF} \bullet |I_{F(120Hz)}| \quad (18)$$

where the setting N_{SF} is the effective ratio between the two currents for a healthy machine.

Comparing the operating and restraining signals (17) and (18) using a fixed slope per (3) results in the operating characteristic shown by green lines in Fig. 19 for a slope setting value of 20 percent. The restraining region is located between the green lines, and the operating region is the area outside the restraining region.

The currents involved in (17) and (18) are in primary amperes or properly matched secondary amperes. The $I_{2(60Hz)}$ phasor is calculated using a filter tuned to the fundamental system frequency. The $I_{F(120Hz)}$ phasor is extracted using a filter tuned to double the system frequency. For accuracy, the two filters work on frequency-tracked samples or use an equivalent method to make the measurements accurate if the frequency changes.

In order to illustrate the operation of the 60SF element using (17) and (18), we simulated an external phase-to-phase fault, followed by a 5 percent turn-to-turn fault in our sample 13.8 kV, 200 MW machine loaded at 100 MW. Fig. 22 shows the terminal voltages and currents and the field current. Fig. 23 shows the I_2 and I_F magnitudes and their ratio. The ratio stays at 13.4 during the external fault as expected and changes dramatically to about 6 when the turn-to-turn fault occurs 5 cycles after the external fault. Fig. 24 shows this case on the operating-restraining current plane per (17) and (18) with a slope setting of 20 percent. The trajectory first settles in the restraining region in response to the external fault and moves into the operating region once the turn-to-turn fault occurs.

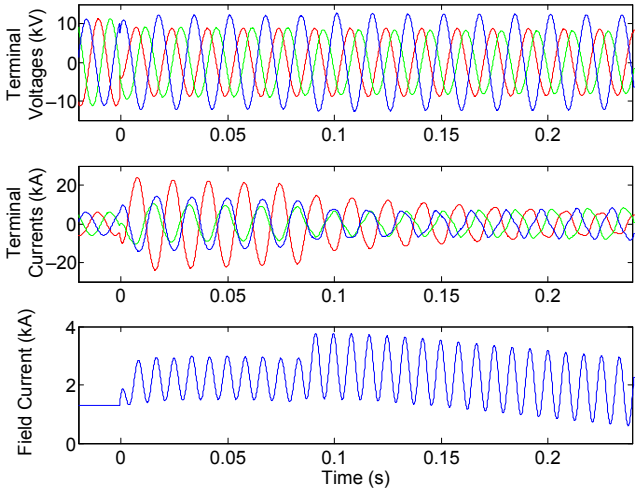

Fig. 22. Evolving external-to-internal fault: terminal voltages and currents and field current.

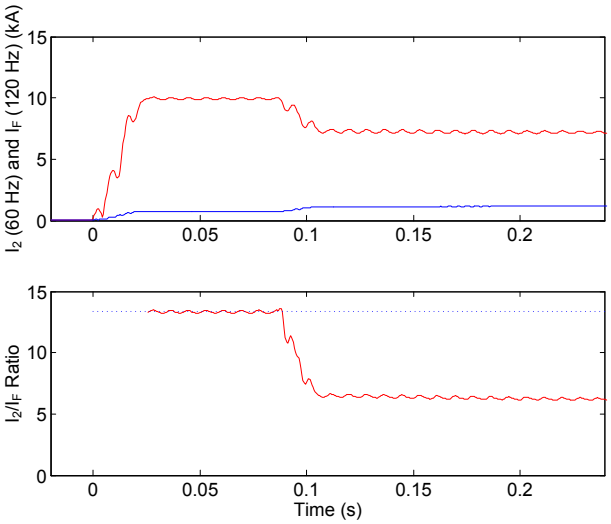

Fig. 23. Evolving external-to-internal fault: negative-sequence current magnitude (60 Hz) in red, field current magnitude (120 Hz) in blue, and their magnitude ratio.

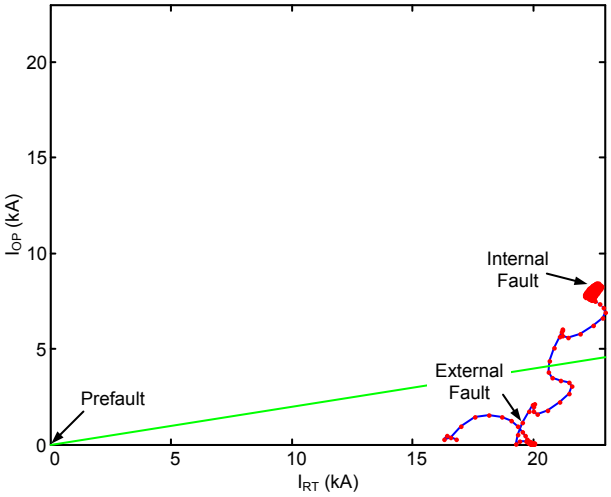

Fig. 24. Evolving external-to-internal fault: fault trajectory on the operating-restraining current plane per (17) and (18).

C. Stator-Rotor Current Differential (87SF) Element

So far, we only used magnitudes of the two currents involved in the AT balance between the rotor and the stator. Can we develop a differential element using the machine stator and rotor phasors and gain more sensitivity as compared with using just the magnitudes? How much sensitivity can we gain?

We have to solve the following two challenges to establish a phasor-based differential element:

- First, the two compared currents are of different frequencies and their phasors rotate at different angular velocities (i.e., at the system frequency and double the system frequency).
- Second, the rotor takes different positions with respect to the stator depending on the output power. Therefore, the phase shift between the two currents depends on the output power.

The first challenge can be solved by slowing down the field current double-frequency phasor by multiplying it by a unity vector that rotates at the system frequency in the negative direction (demodulating with the system frequency). One simple implementation of this principle is to use the positive-sequence voltage phasor as follows:

$$\mathrm{I_{F(60Hz)}} = \mathrm{I_{F(120Hz)}} \bullet \frac{|\mathrm{V_1}|}{\mathrm{V_1}} \tag{19}$$

The advantages of using (19) are that we do not need to use the frequency explicitly and the calculation is correct even as the frequency changes slightly during faults.

Our simulations show that to ensure proper phase relationships between the two compared currents for external unbalances, we need to shift the field current given by (19) by the following angle:

$$\Theta_C = \mathrm{angle}\left(\frac{\mathrm{E_{qPRE}}}{\mathrm{V_{1PRE}}}\right) + \frac{\pi}{2} \tag{20}$$

where $\mathrm{V_{1PRE}}$ is the predisturbance positive-sequence voltage (captured using simple disturbance detection) and:

$$\mathrm{E_{qPRE}} = \mathrm{V_{1PRE}} + \mathrm{jX_d} \bullet \mathrm{I_{1PRE}} \tag{21}$$

where $\mathrm{I_{1PRE}}$ is the predisturbance positive-sequence current and $\mathrm{X_d}$ is the generator direct axis reactance.

In other words, when using $\mathrm{V_1}$ for demodulation in (19), we need to rotate the current by the angle between $\mathrm{V_1}$ and $\mathrm{E_d}$. This angle equals the angle between $\mathrm{V_1}$ and $\mathrm{E_q}$ plus 90 degrees per (20) and (21). We can further combine (20) and (21) and use:

$$\Theta_C = \mathrm{angle}\left(\frac{\mathrm{j} \bullet \mathrm{V_{1PRE}} - \mathrm{X_D} \bullet \mathrm{I_{1PRE}}}{\mathrm{V_{1PRE}}}\right) \tag{22}$$

In order to be able to use (19) and (22), we need to use voltage signals in addition to the current signals and we need to capture the prefault values of the stator voltages and currents. We also need to know the generator direct axis reactance. These requirements make the 87SF element more involved than the simpler 60SF element.

Fig. 25 shows the properly aligned currents for the evolving fault case of Fig. 22. As expected, the two currents are equal in magnitude and out of phase for the external fault. Once the internal turn-to-turn fault occurs 5 cycles later, both the magnitude and the phase relationships become upset, allowing for sensitive fault detection.

A simple implementation of the 87SF element uses the following differential signal:

$$\mathrm{I_{DIF}} = \left|\mathrm{I_{2(60Hz)}} + \mathrm{N_{SF}} \bullet \mathrm{I_{F(60Hz)}} \bullet 1\angle -\Theta_C\right| \tag{23}$$

and the following restraining signal:

$$\mathrm{I_{RST}} = \left|\mathrm{I_{2(60Hz)}} - \mathrm{N_{SF}} \bullet \mathrm{I_{F(60Hz)}} \bullet 1\angle -\Theta_C\right| \tag{24}$$

Comparing the operating and restraining signals (23) and (24) in a slope equation of the type of (3) results in a typical percentage differential characteristic.

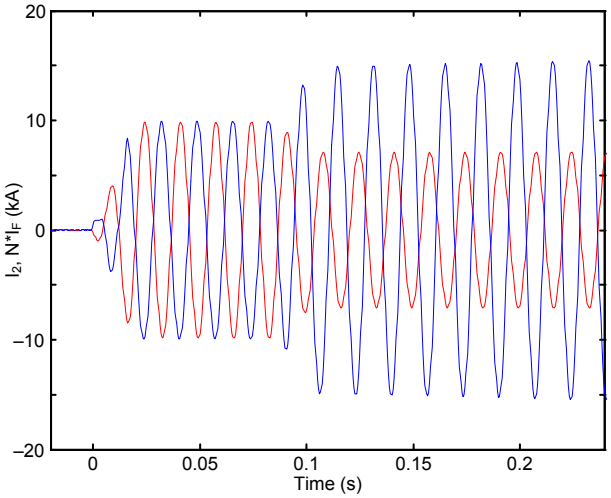

Fig. 25. Evolving external-to-internal fault: filtered negative-sequence stator current (red) and ratio- and frequency-matched and angle-corrected field current (blue).

Fig. 26 shows the block diagram of the 87SF element.

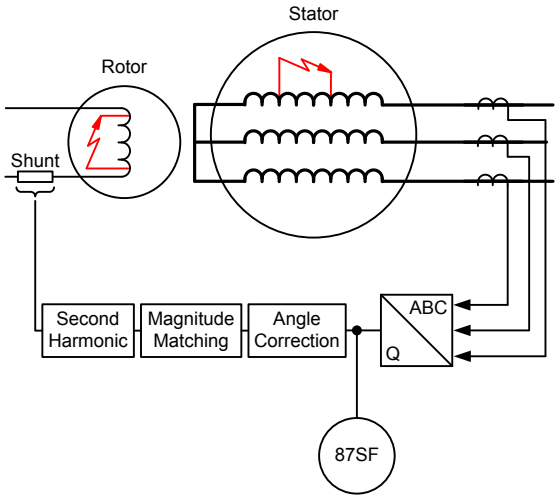

Fig. 26. The 87SF turn-to-turn fault protection element for synchronous generators.

Fig. 27 shows a trajectory of the evolving fault of Fig. 22 on the differential-restraining plane per (23) and (24) with a 20 percent slope setting. When the external fault occurs, the restraining signal increases to about 20 kA while the differential signal is very low. When the turn-to-turn fault occurs after 5 cycles, the differential signal increases to about 8 kA, yielding a reliable operation for this 5 percent turn-to-turn fault, despite the preexisting external fault.

Comparing Fig. 24 (60SF) and Fig. 27 (87SF), we conclude that the two elements behave in a similar fashion, with the 87SF element having a slightly higher operating signal. This is because the phase angle between the two currents does not change much for this turn-to-turn fault (Fig. 25). If the phase angle changed more, the operating signal of the 87SF element would be even higher than that of the 60SF element. According to our simulations, differences in favor of the 87SF element are more visible for turn-to-turn faults on a heavily loaded machine.

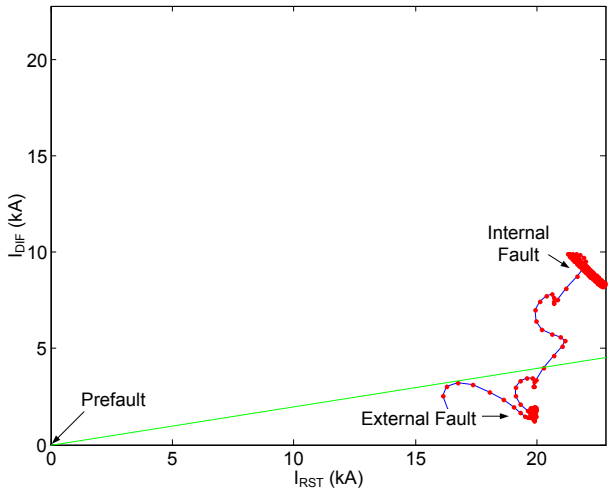

Fig. 27. Evolving external-to-internal fault: fault trajectory on the differential-restraining current plane per (23) and (24).

For completeness, we also used the evolving fault example of Fig. 22 to illustrate the operation of the 32Q element introduced in Section VI. With the external fault present, the apparent impedance does not move to the first quadrant when the stator turn-to-turn fault occurs (Fig. 28). The 32Q element fails to detect the turn-to-turn fault under the presence of an external fault because the external fault impedance dominates over the turn-to-turn fault impedance. This is expected and should not be considered a major limitation. The 60SF and 87SF elements, however, do not have difficulties with this challenging simultaneous external and internal fault case.

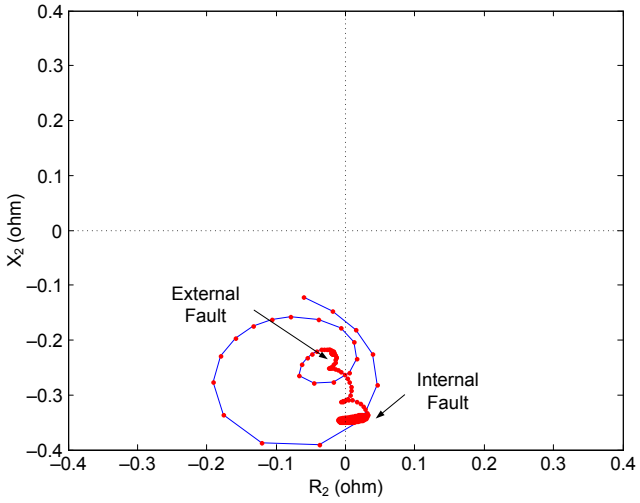

Fig. 28. Negative-sequence apparent impedance measured at the generator terminals for the evolving fault of Fig. 22. Under the preexisting external fault, the apparent impedance does not move to the first quadrant when the turn-to-turn fault occurs.

D. Discussion of 60SF and 87SF Elements

In the previous subsections, we introduced two novel principles for turn-to-turn fault protection of synchronous machines. These principles have been validated with digital RTDS simulations and in a physical generator model. Much work is still needed to gain full confidence in the two protection principles.

At this time, we offer the following comments:

- Both the 60SF and 87SF elements are extensions of the 87Q element, because they balance the negative-sequence current in the stator against the resulting second-harmonic current in the field winding.
- The 60SF and 87SF elements are very sensitive and detect both stator and rotor turn-to-turn faults. Detection of rotor turn-to-turn faults requires an external current unbalance such as an open phase or a fault to create the negative-sequence driving signal.
- The 60SF and 87SF elements are based on the assumption that the ratio between the damper current and the field current is constant. This is true if the impedances of the damper and field circuits at double system frequency are constant. More research is needed to validate this assumption and develop methods to deal with any variability.
- The 60SF and 87SF elements are based on the assumption that the exciter does not produce any double-frequency voltage during normal operation. This is a justified assumption, because the double-frequency current in the field would induce a stator negative-sequence current and a damper current. However, more research is needed to validate this assumption for practical exciter designs.
- The 60SF element is simpler than the 87SF element because it does not require frequency and angle correction. The two elements behave in a similar fashion for small turn-to-turn faults. However, the 87SF element is slightly more sensitive, especially for heavily loaded machines.
- The 60SF and 87SF elements need a slight time delay (1 to 2 cycles) to deal with transient differences between the measurements of the two compared currents. These transient differences are expected because the two measurements use different filters (60 Hz and 120 Hz).
- The 60SF and 87SF elements are susceptible to CT saturation errors for external faults and need proper EFD logic. The EFD logic of Fig. 4 will assert on internal turn-to-turn faults. One simple solution is to use the differential and restraining signals of the 60SF or 87SF elements as the inputs to the Fig. 4 logic.

VIII. Conclusion

87Q protection elements have a good track record when applied to transmission lines and power transformers. Their sensitivity is better than that of 87P elements because they do not overrestrain their operation with the positive-sequence load current. This advantage is also a potential weakness. During balanced external faults, 87Q elements work with a small or zero restraining signal and they need EFD or CT saturation logic for security.

Negative sequence is a natural incremental quantity that develops from zero or small standing values when a fault occurs. This leads to a number of advantages in applications to transmission lines. For example, 87LQ elements are less affected by current misalignment due to asymmetrical channels or by line charging current than are 87LP elements.

The negative-sequence network is typically very homogeneous, and as a result, the negative-sequence currents are almost perfectly in phase for internal faults and out of phase for external faults. This allows for better setting margins and ensures good performance.

When applied to power transformers, 87Q elements detect turn-to-turn faults because they monitor the AT balance of the protected transformer and respond to any event (including turn-to-turn faults) that upsets this balance. 87TP elements also detect transformer turn-to-turn faults, but 87TQ elements are more sensitive due to their lower restraining signals, which do not contain load current.

Unlike the case of power transformers, 87Q elements applied to reactors and stators do not monitor the AT balance of the protected apparatus and are therefore blind to turn-to-turn faults.

This paper proposes the application of 32Q elements for turn-to-turn fault protection in stators and reactors. Especially in applications to stators, 32Q elements are easy to set due to a relatively small variability in the system impedance (owing to the fixed step-up transformer impedance).

This paper derives and explains two novel protection elements for generator turn-to-turn fault protection: 60SF and 87SF. These elements are based on the AT balance between the fields created by the stator negative-sequence current and the rotor double-frequency current. The two elements allow the elimination of damper current measurements and therefore can be practically applied as long as the impedances of the field and damper windings are constant.

The two elements can be considered novel versions of the 87Q principle with the difference that they balance the negative-sequence currents not between the terminal- and neutral-side stator currents, but between the stator negative-sequence current and the double-frequency component of the field current.

The two elements are very sensitive to turn-to-turn faults and detect both stator and rotor turn-to-turn faults.

IX. Acknowledgment

The authors acknowledge Mr. Doug Taylor of Schweitzer Engineering Laboratories, Inc. for his assistance in digital simulations and work on a physical generator model.

X. References

[1] J. Roberts, D. Tziouvaras, G. Benmouyal, and H. J. Altuve, "The Effect of Multiprinciple Line Protection on Dependability and Security," proceedings of the 55th Annual Georgia Tech Protective Relaying Conference, Atlanta, GA, May 2001.

[2] M. J. Thompson, H. Miller, and J. Burger, "AEP Experience With Protection of Three Delta/Hex Phase Angle Regulating Transformers," proceedings of the 60th Annual Conference for Protective Relay Engineers, College Station, TX, March 2007.

[3] A. Guzmán, N. Fischer, and C. Labuschagne, "Improvements in Transformer Protection and Control," proceedings of the 62nd Annual Conference for Protective Relay Engineers, College Station, TX, March 2009.

[4] Z. Gajić, I. Brnčić, B. Hillström, F. Mekić, and I. Ivanković, "Sensitive Turn-to-Turn Fault Protection for Power Transformers," proceedings of the 32nd Annual Western Protective Relay Conference, Spokane, WA, October 2005.

[5] M. J. Thompson, "Percentage Restrained Differential, Percentage of What?," proceedings of the 64th Annual Conference for Protective Relay Engineers, College Station, TX, April 2011.

[6] B. Kasztenny, G. Benmouyal, H. J. Altuve, and N. Fischer, "Tutorial on Operating Characteristics of Microprocessor-Based Multiterminal Line Current Differential Relays," proceedings of the 38th Annual Western Protective Relay Conference, Spokane, WA, October 2011.

[7] Y. Xue, B. Kasztenny, D. Taylor, and Y. Xia, "Line Differential Protection Under Unusual System Conditions," proceedings of the 39th Annual Western Protective Relay Conference, Spokane, WA, October 2012.

[8] G. Benmouyal and T. Lee, "Securing Sequence-Current Differential Elements," proceedings of the 31st Annual Western Protective Relay Conference, Spokane, WA, October 2004.

[9] H. J. Altuve, N. Fischer, G. Benmouyal, and D. Finney, "Sizing Current Transformers for Line Protection Applications," proceedings of the 66th Annual Conference for Protective Relay Engineers, College Station, TX, April 2013.

[10] H. J. Altuve Ferrer and E. O. Schweitzer, III (eds.), *Modern Solutions for Protection, Control, and Monitoring of Electric Power Systems*. Schweitzer Engineering Laboratories, Inc., Pullman, WA, 2010.

[11] H. Miller, J. Burger, N. Fischer, and B. Kasztenny, "Modern Line Current Differential Protection Solutions," proceedings of the 63rd Annual Conference for Protective Relay Engineers, College Station, TX, March 2010.

[12] B. Kasztenny, M. Thompson, and N. Fischer, "Fundamentals of Short-Circuit Protection for Transformers," proceedings of the 63rd Annual Conference for Protective Relay Engineers, College Station, TX, March 2010.

[13] J. Mraz, J. Pomeranz, and J. Law, "Limits of Sensitivity for Detecting Inter-Turn Faults in an Energized Power Transformer," proceedings of the 34th Annual Western Protective Relay Conference, Spokane, WA, October 2007.

[14] N. Fischer, D. Finney, and D. Taylor, "How to Determine the Effectiveness of Generator Differential Protection," proceedings of the 67th Annual Conference for Protective Relay Engineers, College Station, TX, March 2014.

[15] F. K. Basha and M. Thompson, "Practical EHV Reactor Protection," proceedings of the 66th Annual Conference for Protective Relay Engineers, College Station, TX, April 2013.

[16] IEEE Standard C37.102, IEEE Guide for AC Generator Protection.

[17] IEEE Standard C37.109, IEEE Guide for the Protection of Shunt Reactors.

[18] IEEE Standard C37.99, IEEE Guide for the Protection of Shunt Capacitor Banks.

[19] S. Samineni, C. Labuschagne, and J. Pope, "Principles of Shunt Capacitor Bank Application and Protection," proceedings of the 63rd Annual Conference for Protective Relay Engineers, College Station, TX, March 2010.

[20] A. B. Dehkordi, A. M. Gole, and T. L. Maguire, "Real Time Simulation of Internal Faults in Synchronous Machines," proceedings of the 7th International Conference on Power System Transients, Lyon, France, June 2007.

XI. Biographies

Bogdan Kasztenny is the R&D director of technology at Schweitzer Engineering Laboratories, Inc. He has over 25 years of expertise in power system protection and control, including 10 years of academic career and 15 years of industrial experience, developing, promoting, and supporting many protection and control products.

Dr. Kasztenny is an IEEE Fellow, Senior Fulbright Fellow, Canadian representative of CIGRE Study Committee B5, registered professional engineer in the province of Ontario, and an adjunct professor at the University of Western Ontario. Since 2011, Dr. Kasztenny has served on the Western Protective Relay Conference Program Committee. Dr. Kasztenny has authored about 200 technical papers and holds 20 patents.

Normann Fischer received a Higher Diploma in Technology, with honors, from Technikon Witwatersrand, Johannesburg, South Africa, in 1988; a BSEE, with honors, from the University of Cape Town in 1993; and an MSEE from the University of Idaho in 2005. He joined Eskom as a protection technician in 1984 and was a senior design engineer in the Eskom protection design department for three years. He then joined IST Energy as a senior design engineer in 1996. In 1999, Mr. Fischer joined Schweitzer Engineering Laboratories, Inc., where he is currently a fellow engineer in the research and development division. He was a registered professional engineer in South Africa and a member of the South African Institute of Electrical Engineers. He is currently a senior member of IEEE and a member of ASEE.

Héctor J. Altuve received his BSEE degree in 1969 from the Central University of Las Villas in Santa Clara, Cuba, and his Ph.D. in 1981 from Kiev Polytechnic Institute in Kiev, Ukraine. From 1969 until 1993, Dr. Altuve served on the faculty of the Electrical Engineering School at the Central University of Las Villas. From 1993 to 2000, he served as professor of the Graduate Doctoral Program in the Mechanical and Electrical Engineering School at the Autonomous University of Nuevo León in Monterrey, Mexico. In 1999 through 2000, he was the Schweitzer Visiting Professor in the Department of Electrical Engineering at Washington State University. Dr. Altuve joined Schweitzer Engineering Laboratories, Inc. (SEL) in January 2001, where he is currently a distinguished engineer and dean of SEL University. He has authored and coauthored more than 100 technical papers and several books and holds four patents. His main research interests are in power system protection, control, and monitoring. Dr. Altuve is an IEEE senior member.

Previously presented at the 2015 Texas A&M Conference for Protective Relay Engineers.

20150210 • TP6659-01